PERGAMON

International Journal of Heat and Mass Transfer 42 (1999) 4235–4252

International Journal of HEAT and MASS TRANSFER

www.elsevier.com/locate/ijhmt

Mathematical and experimental modelling of quenching a self-propagating high-temperature synthesis process

B.M. Khusid[a,*], V.V. Kulebyakin[a], E.A. Bashtovaya[a], B.B. Khina[b]

[a] *Academic Scientific Complex, A.V. Luikov Heat and Mass Transfer Institute, National Academy of Sciences of Belarus, Minsk 220072, Byelorussia*

[b] *Belarussian State Polytechnic Academy, Minsk, Byelorussia*

Received 14 December 1997

Abstract

The problem of quenching a material in self-propagating high-temperature synthesis (SHS) in flat samples of a titanium–carbon mixture is studied theoretically and experimentally. Possible cooling rates with different ways of heat removal are estimated mathematically. A method of quenching by a high-velocity impinging jet is chosen. The method provides the conditions of heat removal necessary for stopping the combustion wave front (a rate of temperature decrease $\simeq 10^4$ K s^{-1} for a 2-mm-thick specimen). A mathematical model of material quenching in the process of SHS is developed for one- ($A \rightarrow B$) and two-stage ($A \rightarrow B \rightarrow C$) reactions. Thermal processes and composition of material in stopping the front in a flat plate sample of a titanium–carbon mixture is studied numerically on the basis of the model proposed. The dependence of the cooling rate on temperature in different zones of an SHS-wave are calculated; in this case a two-stage reaction is considered to occur in the so-called fusion, control, and separation modes. A schematic diagram of an experimental setup and results of experimental study of the proposed model of quenching are given. Feasibility of using the method of quenching by an impinging jet is demonstrated for studying the processes of phase and structure formation during the SHS.

1. Introduction

Self-propagating high-temperature synthesis (SHS) occupies a special place among various physiochemical processes of producing modern inorganic materials (heat-resistant and heat-proof, superhard and wear-resistant, insulating, etc.). The advantages of SHS are low energy consumption, simplicity of equipment, high efficiency and purity of products. In this case heat transfer and kinetics of chemical, phase, and structural transformations are of considerable scientific interest since the process is characterized by high temperatures in a condensed phase, high heat capacities of products, low constants of mass transfer in combination with high rates of chemical reactions, and by a specific multistage nature of phase and chemical transformations [1–6]. At present the mechanisms of this process are intensely studied by physicochemical, materiallographic, and thermodynamic methods. A specific feature inherent in SHS is the presence of condensed products forming spatial structures at different stages of the process. These products carry information about the process itself and their analysis gives information on the mechanism of SHS. Usually the composition and structure of the products are studied after an SHS-wave has passed and the specimens are

* Corresponding author.

0017-9310/99/$ - see front matter
PII: S0017-9310(99)00062-9

Nomenclature

A	substance
a	thermal diffusivity [$m^2\ s^{-1}$]
c	heat capacity [J $mol^{-1}\ K^{-1}$]
d	diameter [m]
E	activation energy [J g^{-1}]
$e_i=(\lambda_i c_i \rho_1)^{1/2}$	thermal activity [J $m^2\ K^{-1}\ s^{-1/2}$]
$Fo=a\tau_0/l^2$	Fourier number
ΔH_{ev}	heat of evaporation [J kg^{-1}]
$h=(1-K_e)/(1+K_e)$, $K_e=e_1/e_2$	dimensionless complex
k	reaction rate constant [s^{-1}]
$Ki=ql/[\lambda(T_{comb}-T_{cm})]$	Kirpichev number
L	specimen length [m]
$Nu=\alpha L/\lambda$	Nusselt number
p	pressure [Pa]
Pe	Peclet number
$Q=-\Delta H^0$	heat release of a chemical reaction [J kg^{-1}]
q	heat flux [W m^{-2}]
$S=Q/(c_0\Delta T_0)$	dimensionless complex
T	temperature [K]
u	jet velocity [m s^{-1}]
V	volume [m^3]
w	specimen thickness [m]
x, y, z	coordinates in three space directions.

Greek symbols

α	coefficient of heat transfer [W $m^{-2}\ K^{-1}$]
$\beta=RT_{max}/E$	dimensionless complex
ε	porosity ($\rho_{ch}(1-\varepsilon_{ch})=\rho_{pr}(1-\varepsilon_{pr})$)
η	degree of conversion
θ_0	relative temperature
λ	thermal conductivity [W $m^{-1}\ K^{-1}$]
μ_n	characteristic numbers
$\nu_x=l_0^2/x_0^2$, $\nu_y=l_0^2/y_0^2$	dimensionless complexes
$\xi=E\Delta T_0/(RT_{max}^2)$	dimensionless complex
ρ	density [kg m^{-3}]
τ	time [s]

Subscripts

ad	adiabatic
boil	boiling
ch	charge
cm	cooling medium
comb	combustion
cr	critical
ev	evaporation
f	final
fr	front of combustion
$i=1, 2$	sample and substance-coolant, respectively
ig	ignition
liq	liquid
max	maximum
melt	melting

pr	product
r	chemical reaction
sat	saturation
sc	scaling
0	initial state.

cooled. In this case the processes of thermal, chemical, and concentration relaxation are accomplished and the content of nonreacted substances in the SHS-products is usually low, because the synthesis is characterized by a high degree of conversion. At the same time, in various zones of the synthesis wave (which have different temperatures) the starting reactants, intermediate phases, and final products of combustion are present simultaneously. The information of the product formation processes can be obtained if we arrest a state of the combustion wave by sharp cooling of the system. In this case, however, it is well to bear in mind the fact that the heat balance, value and direction of temperature gradients, spatial distribution of the heat release rate will change during highly intense cooling of the specimen. This poses the question on the conformity of the high-temperature and quenched states.

The required cooling rate is $\sim 10^4$–10^5 K s^{-1}. The existing means of cooling of specimens with the SHS process occurring in them give insufficiently high cooling rates [1–3]. For liquid metals and alloys, the melt quenching (MQ) methods are used which allow one to obtain microcrystalline and amorphous materials [7]. Rolling between rotating rolls, melt spinning, flattening of a droplet between cooled copper plates, high-speed spraying by liquids and gases provide quenching rates $\sim 10^4$–10^7 K s^{-1}, but they are not acceptable for SHS specimens because they cause destruction of the shape and structure of materials.

Along with the mentioned quenching methods, fast cooling of a liquid or gas by an impinging jet is widely used in metallurgy and power engineering. The advantages of the method are high intensity of heat transfer and simplicity of control of its characteristics. A great number of works [17,42–45], the results of which indicate the possibility of fast cooling by this method, are devoted to the processes of interaction between an impinging jet and a hot surface under the conditions of one-phase convective heat transfer and vaporization.

In the paper, mathematical modelling of heat transfer, chemical and phase transformations, the evolution of temperature fields, heat release rate and cooling rate during quenching of a burning SHS-specimen by an impinging jet is carried out. The process of quenching is implemented experimentally.

2. Estimation of heat removal rates from the surface of an SHS-specimen by different methods

Fast cooling of a body heated to high temperatures without substantial changes of its shape and structure can be attained by

- conductive heat removal into a material with high thermal conductivity;
- evaporating a liquid coolant on a surface;
- intense convective heat transfer.

2.1. Conductive heat removal

We estimate a maximum quenching rate using heat removal from an SHS specimen into a massive copper bar. An ideal thermal contact can be attained by depositing a thin film of a low-melting high-boiling metal, e.g., indium ($T_{melt}=156°C$, $T_{boil}=2060°C$ [8]). A time of heating an indium film with a thickness $l\sim 1$ μm to the fusion point $\tau\sim l^2/a\sim 10^{-2}$ s at thermal diffusivity $a\approx 0.3$ cm^2 s^{-1} [9] is rather small. This process is described within a framework of a conjugate problem of heat transfer for two contacting bodies. The solution of the problem is given in [10]. For two-sided cooling of a flat specimen with a half-thickness l a relative decrease in temperature at the center $\theta_0=(T_f-T_{cm})/(T_{comb}-T_{cm})$ will be found by the formula [10]

$$\theta_0 = 1 - \frac{2}{K_e+1}\sum_{n=1}^{\infty}(-h)^{n-1}\mathrm{erfc}\frac{(2n-1)l}{2\sqrt{a_1\tau}}, \qquad (1)$$

where $h=(1-K_e)/(1+K_e)$, $K_e=e_1/e_2$, $e_i=(\lambda_i c_i\rho_i)^{1/2}$ is the thermal activity (for copper $e_2=36.4$ kJ m^{-2} K^{-1} s$^{-1/2}$ [8]).

For quantitative estimates we consider formation of TiC in SHS in the Ti–C system. Thermophysical parameters of this system ($T_{comb}=2500$–$3000°C$) are typical of the majority of SHS-processes in the metal–carbon and metal–boron systems. The rate of cooling to $T_f=500°C$ when reactions and phase transformations in the Ti–C system are terminated should be not less than $\sim 10^4$K s^{-1}. Then the time of cooling $\tau_0=(T_{comb}-T_f)/V_0\sim 0.1$ s and a relative decrease in temperature is $\theta_0=0.16$–0.20. For titanium carbide

with thermophysical parameters $\lambda = 30$ W m^{-1} K^{-1}, $c_p = 58.6$ J mol^{-1} K^{-1}, $\rho = 4.93$ g cm^{-3} [11], at the center of the plate with $l = 2$ mm during the time 0.1 s formula (1) gives $\theta_0 \approx 0.8$. The rate of temperature decrease in this case is $\sim 10^3$ K s^{-1}.

Consequently, conductive heat removal with an ideal two-sided contact of a cooled copper block with the specimen provides a rate of quenching not higher than 10^3 K s^{-1}.

2.2. Liquid-droplet evaporation

Evaporation cooling of liquid on the specimen surface corresponds to the second-order boundary conditions, i.e., the constancy of a heat flux. For two-sided cooling of the plate with a half-thickness l, a relative decrease in temperature at the center is determined by the relation [10]

$$\theta_0 = 1 - Ki\left(Fo - \frac{1}{6}\right) + \sum_{n=1}^{\infty}(-1)^{n+1}\frac{2}{\mu_n^2}$$

$$\exp(-\mu_n^2 Fo), \qquad (2)$$

where μ_n are the characteristic numbers. The value $\theta_0 = 0.16$–0.20 at the center of the plate is attained at a very large value of the heat flux $q \sim 10$ kW cm^{-2}. This heat flux can be attained in the mode of liquid-droplet evaporation of a low-melting metal (for sodium $T_{melt} = 98$°C, $T_{boil} = 882$°C, evaporation heat $\Delta H_{ev} = 99$ kJ mol^{-1} at $T = T_{boil}$; for potassium $T_{melt} = 63$°C, $T_{boil} = 779$°C, $\Delta H_{ev} = 79$ kJ mol^{-1} at $T = T_{boil}$ [12,13], Wood alloys of the systems Bi–Pb–Sn, Bi–Pb–Sn–Cd ($T_{melt} = 68$–140°C), or a cryogenic coolant.

We make estimates for sodium which possesses, compared to potassium, a lower chemical activity, higher thermal conductivity $\lambda = 52$ W m^{-1} K^{-1} at $T = 827$ K [12,14], and higher values of evaporation heats at T_{boil} and of a critical temperature $T_{cr} = 2230$°C, $p_{cr} = 25$ MPa [13,14]. Among cryogenic fluids we consider argon: $T_{cr} = -122$°C, $p_{cr} = 4.8$ MPa, $T_{boil} = -185.9$°C, $\Delta H_{ev} = 2.6$ kJ mol^{-1} at $T = -128$°C. In a limiting case of evaporation to vacuum with continuous supply of coolant, a mass rate of evaporation can be estimated by the Hertz–Knudsen formula $w = p/(2\pi RT/\mu)^{1/2}$. It amounts to 6.3 g cm^{-2} s^{-1} for sodium at the boiling temperature and $W \sim 1000$ g cm^{-2} s^{-1} for argon $T = -128$°C. Then the heat flux due to evaporation of the coolant attains a value of 27 kW cm^{-2} for argon that exceeds a required value of the heat flux $q \sim 10$ kW cm^{-2}.

For one-sided cooling of a flat specimen with a thickness $l = 2$ mm from $T_{comb} = 3000$°C to the boiling point of sodium (779°C) an amount of heat equal to

$$\Delta H = \int_{T_{boil(Na)}}^{T_{comb}} c_p(T)\,dT\,l\,\rho_{TiC} = 1.8 \text{ kJ cm}^{-2}$$

should be removed from the unit surface. In this case 0.5 g of sodium at $T = T_{boil}$ or 30 g of argon at $T = -128$°C will evaporate. The time of evaporation will amount to 0.1 s for sodium or ~ 0.05 s for liquid argon, i.e., it does not limit the process of cooling.

Taking a minimum diameter of droplets in spraying liquid coolant as ~ 0.1 mm, we obtain a time of film heating-up $\tau = d^2/a = 2 \times 10^{-4}$ s for sodium at $a \approx 0.5$ cm^2 s^{-1}. For estimates the values $\rho = 0.754$ g cm^{-3}, $c_p = 29$ J mol^{-1} K^{-1} at $T = 800$°C were taken [13–15]. The calculated time of heating-up of the whole mass of sodium is rather small ~ 0.01 s. For argon we take thermophysical parameters on the saturation line at 140 K $\lambda = 0.07$ W m^{-1} K^{-1}, $c_p = 1.6$ kJ kg^{-1} K^{-1}, $\rho = 1$ g cm^{-3} [15]. In this case the time of heating-up of the evaporated mass of argon is much higher than the required time of specimen cooling ~ 1 s, i.e., the rate of quenching $v_0 > 10^4$ K s^{-1}, but implementation of the liquid-droplet evaporation process is technically difficult because of the necessity of fast dispersion of the coolant and the removal of a large amount of vapours: at the boiling temperature a volume of vapour will amount to $V = mRT/(p\mu) \sim 10^3$ cm^3 cm^{-2} of the specimen surface.

2.3. Convective heat transfer

A convective mode of heat transfer corresponds to the third-kind boundary conditions on the specimen surface. According to the nomograms relating the Biot and Fourier numbers at $\tau_0 \sim 0.1$ s and the characteristic thickness of the specimen $l = 2$ mm [10] a relative decrease in temperature $\theta_0 = 0.16$–0.20 is attained at a value of the coefficient of heat transfer $\alpha \sim 10^4$–10^5 W m^{-2} K^{-1}. In a longitudinal turbulent flow of liquid sodium past a plate of a length L the Nusselt number is $Nu = \alpha L/\lambda \approx 0.4 Pe^{0.65}$ [14]. To provide $\alpha \sim 10^5$ W m^{-2} K^{-1} at $T = 1200$°C we need a value of the Peclet number $Pe \approx 1.3 \times 10^5$ and, respectively, the velocity of a sodium jet $u \approx 120$ m s^{-1}. This value exceeds the velocity necessary for stalling a vapour layer. For a jet of liquid argon $Nu \approx 0.37 Re^{0.8} Pr^{0.43}$ and a value of the coefficient of heat transfer $\alpha \sim 10^5$ W m^{-2} K^{-1} is attained at the flow velocity $u \approx 150$ m s^{-1} at a critical temperature that is also higher than the velocity of vapour layer stalling. Similar estimates for a Wood alloy (55% Bi + 45% Pb, $T_{melt} = 123$°C) at 700°C show that $\alpha \sim 10^5$ W m^{-2} K^{-1} is attained by $u = 155$ m s^{-1}. By virtue of this it is expedient to employ a convective mode of cooling in the flow of a liquid coolant, a dynamic head of which can provide stalling of a

vapour layer: $\rho u > p_{sat}$, where u is the jet velocity, p_{sat} is the pressure of saturated vapour. For a sodium flow $u = 12$ m s^{-1} at T_{boil}, $u = 40$ m s^{-1} at $T = 1200$°C. In the case of a liquid argon jet $u = 100$ m s^{-1} at $T = T_{cr}$.

However, use of the mentioned media under the conditions of SHS is technically very difficult. This makes one prefer a high-speed water jet. Without regard for heat of the liquid–vapour phase transition the coefficient of heat transfer at a point of water jet impingement on an obstacle is found from the relation $Nu = 1.5Re^{0.5}Pr^{0.4}$. A value of $\alpha \geq 10^4$ W m^{-2} K^{-1} for a jet issuing from the nozzle with a diameter 2 mm is attained at $u \geq 150$ m s^{-1} [16,17]. This is higher than the velocity necessary for stalling a vapour layer. A real value of the coefficient α should be even higher because of evaporation of water on the cooled surface and vapour entrainment by a high-speed jet.

3. Mathematical model and numerical calculation

3.1. Physical formulation of the problem

A specimen is in the form of a rectangular plate a thickness w of which is much smaller than longitudinal dimensions: a length l and a width z. The position of coordinates is shown in Fig. 1a.

The specimen is ignited by a wall heated to a temperature $T_{ig} = T_{ad}$ ($x = 0$) during the time of initiation t_{ig}, where the adiabatic temperature $T_{ad} = T_0 + Q/c$ is determined by an initial temperature T_0 and heat release of a chemical reaction $Q = -\Delta H^\circ$. After establishment of a stationary combustion mode at $t = t_j$, cooling by a high-speed water jet directed along the normal to the side $Y = 0$ begins (Fig. 1a). Due to a small size of the specimen the conditions of cooling are supposed to be equal over the entire surface.

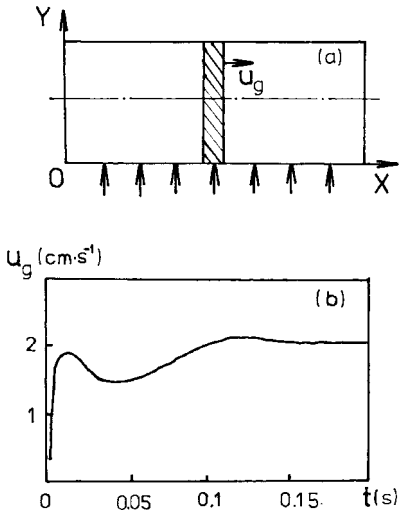

Fig. 1. Schematic of a computational region (a) and attainment of a stationary mode by the SHS-wave (b).

3.2. Model of a one-stage reaction

Variation of temperature and the degree of conversion for a one-stage reaction in an SHS-wave is described by the equations of the theory of thermal combustion of condensed systems [4]. To allow for the effect of the kinetics of heterogeneous reaction on a temperature dependence of the reaction rate we use the first-order model [4]

$$\varphi(\eta) = (1-\eta)^n, \quad n = 1,$$

where η is the degree of conversion, $0 \leq \eta \leq 1$. In the dimensionless variables

$$\theta = (T - T_0)/\Delta T_0, \quad \tau = t/t_0, \quad x = X/x_0, \quad y = Y/y_0,$$

where $\Delta T_0 = T_{sc} - T_0$, T_{sc} is the temperature scale, $T_{sc} \leq T_{ad}$, x_0, y_0, t_0 are the scales along the axes $0x$, $0y$, and the time t; variation of temperature and the degree of conversion is described by the equation

$$\overline{\rho c}\frac{\partial\theta}{\partial\tau} = \nu_x\frac{\partial}{\partial x}\left(\bar{\lambda}\frac{\partial\theta}{\partial x}\right) + \nu_y\frac{\partial}{\partial y}\left(\bar{\lambda}\frac{\partial\theta}{\partial y}\right) + \overline{\rho c}\frac{\partial\eta}{\partial\tau}; \tag{3}$$

$$\frac{\partial\eta}{\partial\tau} = r(1-\eta)^n \exp\left[\frac{(\theta-1)\xi}{1+(\theta-1)\xi\beta}\right] \tag{4}$$

with the initial and boundary conditions

$$\theta(x,y,0) = 0, \quad \eta(x,y,0) = 0,$$

$$x = 0: \quad \theta = \theta_i = S/\bar{c} \text{ for } \tau \leq \tau_i, \quad \partial\theta/\partial x = 0 \text{ for } \tau > \tau_i$$

$$x = L/x_0: \quad \partial\theta/\partial x = 0;$$

$$y = 0: \quad \bar{\lambda}\,\partial\theta/\partial y = 0 \text{ for } \tau \leq \tau_j, \quad \bar{\lambda}\,\partial\theta/\partial y = \bar{\alpha}(\theta\,|_{y=0} - \theta) \text{ for } \tau > \tau_j$$

$$y = W/y_0: \quad \partial\theta/\partial y = 0. \tag{5}$$

In many systems with SHS the dimensions of the specimen virtually do not change, therefore the density may be taken constant. The differences in the densities of the charge ρ_{ch} and the product ρ_{pr} lead to the change in porosity ε: $\rho_{ch}(1-\varepsilon_{ch}) = \rho_{pr}(1-\varepsilon_{pr})$. Due to the difference in heat capacities of the charge and the product in Eq. (3) $\bar{c} = (1-\eta)\bar{c}_{ch} + \eta\bar{c}_{pr}$.

3.3. Substantiation of initial data for a one-stage reaction

Calculations were performed for a model SHS-system in which chemical interaction and thermophysical parameters correspond to the formation of titanium carbide TiC with a stoichiometric ratio of initial components. Interaction between titanium and carbon in an SHS-wave occurs predominantly in a liquid phase [30,35,38]. With this in view, thermophysical parameters of the process were determined for liquid titanium using the data of [11,12,39]. With account for enthalpies of phase transitions and the temperature dependence of heat capacity, a thermal effect of TiC formation from liquid titanium and graphite is equal to 2.92×10^3 kJ kg^{-1} at 298 K, 3.43×10^3 kJ kg^{-1} at 2200 K. The adiabatic combustion temperature in the Ti–C system amounts to 3200 K [28]. Since thermal effects of titanium crystallization ($\approx$70 kJ kg^{-1}) and the $\beta \rightarrow \alpha$-transition (30.5 kJ kg^{-1}) are small compared to the heat of reaction, in calculations of the evolution of thermal fields during quenching these effects were neglected. Thermal conductivity of the product and original charge (a mixture of liquid titanium and graphite (the subscript ch)) was determined by a simple dependence on porosity: $\lambda_{pr} = \lambda_{TiC}(1-\varepsilon_{pr})$, $\lambda_{ch} = \lambda_{Ti(liq)} \times (1-\varepsilon_{ch})$. With the porosity in the initial state equal to 50% [30,38], it amounts to 48% after titanium melting and 67% on completion of the reaction. Thermal conductivity of liquid titanium does not depend on temperature [40,41]. Mean value of thermal conductivity of graphite and titanium carbide at 2200 K were taken in calculations.

According to the data of [30], in SHS of titanium carbide the activation energy under the conditions of interaction between liquid titanium and graphite is 120 kJ mol^{-1}. The preexponential factor k was determined by the Zeldovich–Frank–Kamenetskii formula for the stationary combustion u which for the first-order reaction has the form

$$u^2 = \frac{(2-n)\lambda_0}{\rho_0 Q}\int_{T_0}^{T_{ad}} \exp\left(-\frac{E}{RT}\right)\mathrm{d}T. \qquad (6)$$

At the porosity of the initial mixture 50%, the rate of combustion of the titanium–carbon system is $u \approx 3$ cm s^{-1} [30,38], then $k \approx 2 \times 10^4$ s^{-1}. Choosing $T_{ad} = 1500$ K, $T_0 = 300$ K, $Q = 3.2 \times 10^3$ kJ kg^{-1}, $c_0 = 1$ kJ mol^{-1} K^{-1}, $\rho_0 = 1.8$ g cm^{-3}, we obtain the following values of dimensionless parameters: $S = 2.66$, $\beta = 0.106$, $\xi = 7.515$, $r = 2 \times 10^{-3}$. For a 2-mm-thick specimen the scales $y_0 = x_0 = 0.25$ mm are taken, then $\nu_x = \nu_y = 0.18$, $\bar{\alpha} = 1.25$ and 12.5 at $\alpha = 10^5$ and 10^6 W m^{-2} K^{-1}.

3.4. Numerical studies

The problem, Eqs. (3)–(5) was solved numerically by finite-difference techniques [18] using the fourth-order Runge–Kutta method for Eq. (4), and a conservative implicit finite-difference scheme of the order 0 $(h^2 + \Delta\tau)$, and the method of splitting by directions for a two-dimensional nonlinear equation of heat conduction, Eq. (3).

Numerical modelling of the SHS-process without quenching shows that a stationary mode of combustion with the rate $\approx$2 cm s^{-1} is established at $t = 0.075$ s (Fig. 1b) and the duration of ignition $t_i = 0.02$ s. On this basis we selected the time of the start of quenching $t_j = 0.12$ s when the coordinate of the combustion front $x_{fr} \approx 2$ mm.

After the start of cooling at $\alpha = 10^5$ and 10^6 W m^{-2} K^{-1} a most fast reduction of temperature occurs on a cooled surface $Y = 0$ and the temperature is almost the same within the entire after-burn zone. Along the cross-sections $Y = W/2$ and $Y = W$ temperature decreases much slower and in this case a maximum of the temperature profile lies in the fast-reaction zone where heat release rate is the largest due to the chemical reaction (Fig. 2a). It is convenient to characterize the position and the shape of the combustion front by the quantity

$$\omega(Y, t) = h\int_0^L \eta((X, Y, t)\,\mathrm{d}X,$$

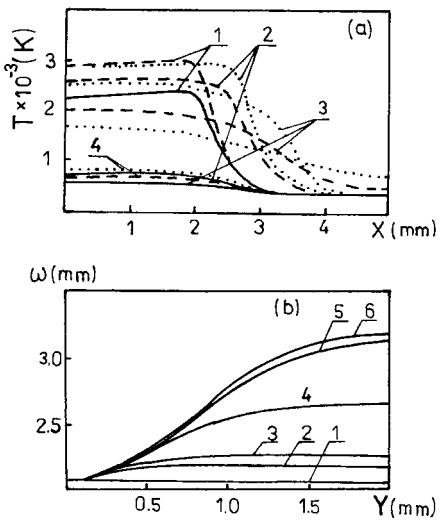

Fig. 2. Distrubution of temperature along a specimen (a) and of a quantity of reacted substances across a specimen (b) in quenching for a one-stage reaction. (a) 1, $t = 0.12$ s; 2, 0.15 s; 3, 0.2 s; 4, 0.5 s; (b) 1, $t = 0.12$ s; 2, 0.125 s; 3, 0.13 s; 4, 0.15 s; 5, 0.2 s; 6, 0.3 s.

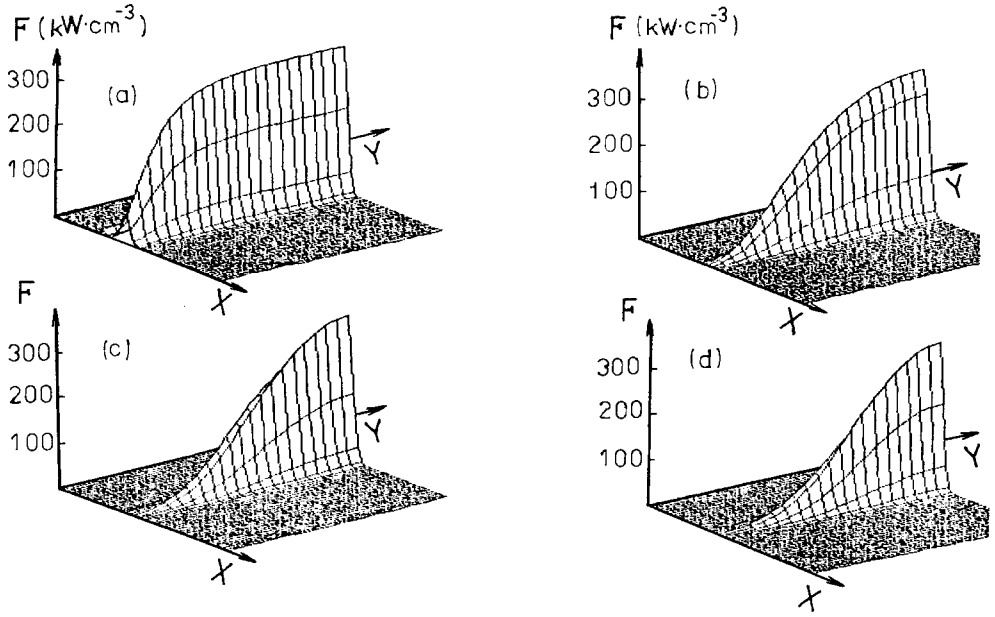

Fig. 3. Evolution of the field of heat release rate in quenching for a one-stage reaction: (a) $t = 0.12$ s; (b) 0.13 s; (c) 0.15 s; (d) 0.2 s.

which has dimensions of a length indicating an amount of the substance burnt (h is the step along the axis $0x$). Combustion quickly stops on the cooled surface $Y = 0$. This leads to bending of the plane front of th SHS-wave (Fig. 2b). The motion of the front ceases in a time $t = 0.18$ s at $\alpha = 10^5$ W m^{-2} K^{-1}. It is convenient to follow the instant of combustion front stopping by a change in the field of heat release rate $F = Q\partial\eta/\partial t$ (Fig. 3). A maximum of the heat release rate is on the specimen surface $Y = W$ and with time it shifts along the axis $0x$. Cessation of the heat release corresponds to stopping of the combustion front.

The rate of temperature decrease $V_0 = \mathrm{d}T/\mathrm{d}t$ changes from $\sim 10^6$ K s^{-1} on the cooled surface to $\sim 10^4$ K s^{-1} on the opposite side of the specimen. Since in melt quenching and heat treatment of metals and alloys a high cooling rate should be attained within a temperature range covering the phase transition points, a diagram of the dependence of V_0 on an instantaneous value of temperature is an important characteristic of quenching conditions. The temperature dependence of the quenching rate for the points lying in different zones of an SHS wave (the preheat, fast-reaction, and after-burn zones) at different distances from the cooled surface are given in Fig. 4. The rate of temperature drop decreases sharply with temperature. In the after-burn zone within the range of temperatures of the melt existence $T = 1900$–3000 K $V_0 \sim 10^4$ K s^{-1} (curves 1–3 in Fig. 4). This provides the possibility to arresting a high-temperature liquid phase. In the fast-reaction zone and near to it, due to continuing heat release, a high rate of temperature drop $V_0 \geq 10^4$ K s^{-1} is attained only at the cooled edge of the specimen (Fig. 4a). The width of the region where a chemical reaction takes place increases with the distance from the cooled surface. In this region heating lasts for some time ($V_0 < 0$ in Fig. 4b, c), but the attained temperature decreases sharply with a distance from the position of the reaction front at the moment of onset of quenching. In the cross-section $X = 3$ mm a maximum value of temperature is 1500 K (below the melting point of titanium) at the center of the specimen and 2300 K on the surface $Y = 2$ mm; the cooling rate is $V_0 \sim 10^4$ K s^{-1}. For $T < 1500$ K $V_0 \sim 10^2$–10^3 K s^{-1} that is commensurable with an ordinary value of the quenching rate for metals and alloys.

Thus, a numerical study of temperature fields in quenching the substance in an SHS-wave by the method suggested in this paper indicates the possibility of the attainment of the cooling rate $V_0 \sim 10^4$ K s^{-1} within a temperature range of the existence of the melt in the titanium–carbon system. This is sufficient to arrest a high-temperature state of substance in the fast-reaction and after-burn zones.

3.5. A model for a two-stage reaction: influence of a stage nature of chemical interaction on heat transfer and structure formation

It should be noted that in many systems the processes have a multistage nature and proceed via the formation of intermediate compounds, metastable

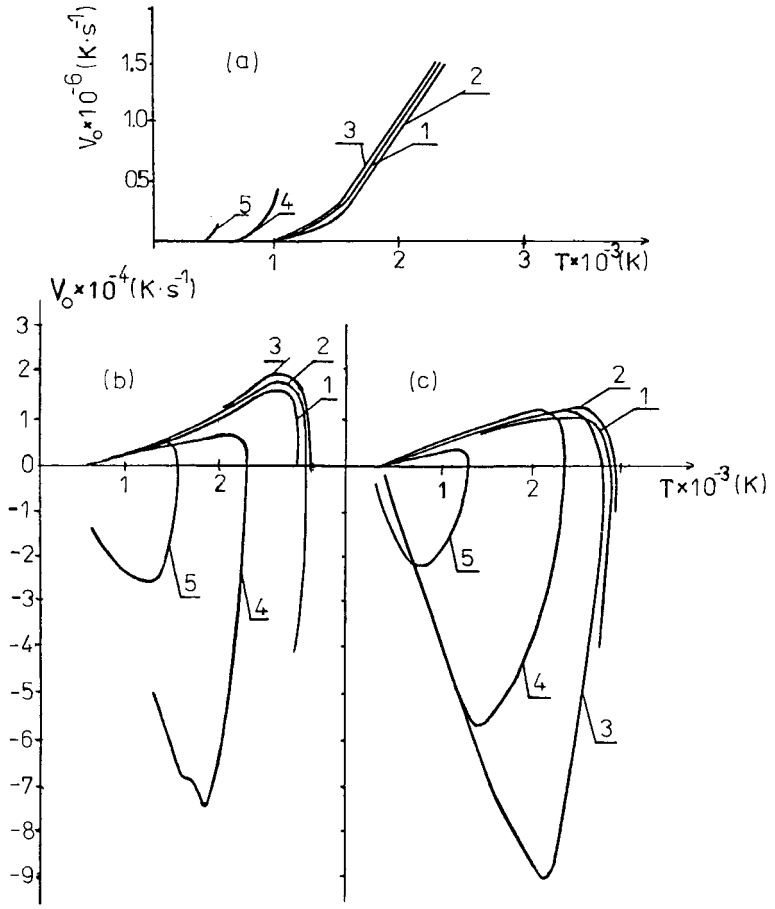

Fig. 4. Dependence of the cooling rate on temperature in different cross-sections of the specimen for a one-stage reaction: (a) $Y = 0$ mm; (b) 1 mm; (c) 2 mm; (1) $x = 1$ mm; (2) 1.5 mm; (3) 2 mm; (4) 2.5 mm; (5) 3 mm.

phases which may be absent in a final structure of the product. Propagation of a combustion wave with consequent two-stage reactions of the type $A_1^I \rightarrow A_2^{II} \rightarrow A_3$ is widely studied in the literature [5,6,19–25, and others].

Depending on the ratio of activation energies and heats of reactions I and II, three modes can occur: the so-called "control", "fusion" and "separation" modes which differ by the distribution of concentrations of intermediate (A_2) and final (A_3) products in the combustion wave. However, in the experiments with SHS these characteristics are not fixed directly in the combustion wave. The modes of control, fusion and slight separation (when a width of the region of an intermediate product is small) differ insignificantly from each other by the temperature profile [19]. Consequently, a temperature profile of the combustion wave determined by the thermocouple technique does not allow one to unambiguously judge the mode of the process.

3.6. Numerical investigations

By virtue of the above, numerical investigations of thermal processes in quenching the material in the SHS-wave in the case of two consequent reactions $A_1^I \rightarrow A_2^{II} \rightarrow A_3$ acquire a large significance. As has been discussed above, the cooling rate $V_0 \approx 10^4$–10^5 K s^{-1} is necessary to arrest a high-temperature state of substance in the SHS-wave and it can be attained using a high-speed water jet directed along the normal to the specimen surface.

We consider combustion of a two-dimensional specimen of a length L and width W. Ignition was performed by a wall heated to a temperature $T_{ig} = T_{ad}$ (at $X = 0$) during time t_{ig}, where $T_{ad} = T_0 + (Q_1 + Q_2)/c$ is the adiabatic combustion temperature, $T_0 = T(X, Y, 0)$ is the initial temperature. Cooling of the specimen by a high-speed water jet directed along the normal to the side $Y = 0$ begins on attainment of the steady-state

mode of combustion (when $t=t_j$). The rate of heat removal from the cooled surface of the specimen is determined by the Newton law. Changes in the temperature field and degrees of conversion for reactions I and II are described by the equations of heat conduction and kinetics. Within the framework of the theory of combustion of condensed systems [4,26] the Arrhenius dependence of the chemical reaction rate on temperature is assumed which account for retardation of reaction by the formed layer of the product by the law $(1-\eta)^n$. For a two-stage reaction in the dimensionless quantities $\theta=(T-T_0)/\Delta T_0$, $\tau=t/t_0$, $x=X/x_0$, $y=Y/y_0$ the problem has the form

$$\overline{\rho c}\frac{\partial\theta}{\partial\tau}=\nu_x\frac{\partial}{\partial x}\left(\bar{\lambda}\frac{\partial\theta}{\partial x}\right)+\nu_y\frac{\partial}{\partial y}\left(\bar{\lambda}\frac{\partial\theta}{\partial y}\right)+\overline{\rho S}\sigma_Q\frac{\partial\eta_1}{\partial\tau}+\overline{\rho S}(1-\sigma_Q)\frac{\partial\eta_2}{\partial\tau}; \tag{7}$$

$$\frac{\partial\eta_1}{\partial\tau}=r_1(1-\eta_1)^{n_1}\ \exp\left[\frac{(\theta-1)\xi\sigma_E}{1+(\theta-1)\xi\beta}\right]; \tag{8}$$

$$\frac{\partial\eta_2}{\partial\tau}=r_2(\eta_1-\eta_2)^{n_2}\ \exp\left[\frac{(\theta-1)\xi(1-\sigma_E)}{1+(\theta-1)\xi\beta}\right] \tag{9}$$

The initial conditions

$$\theta(x,y,0)=0,\quad \eta_1(x,y,0)=0,\quad \eta_2(x,y,0)=0. \tag{10}$$

The boundary conditions for the axis $0X$

$$x=0:\ \theta=\theta_i=S/\bar{c},\ \text{for}\ \tau\le\tau_i,$$

$$x=0:\ \partial\theta/\partial x=0,\ \text{for}\ \tau>\tau_i,$$

$$x=L/x_0:\ \partial\theta/\partial x=0; \tag{11}$$

for the axis $0Y$

$$y=0:\quad \bar{\lambda}\frac{\partial\theta}{\partial y}=0\ \text{for}\ \tau\le\tau_j,$$

$$y=0:\quad \bar{\lambda}\frac{\partial\theta}{\partial y}=\bar{\alpha}(\theta\,|_{y=0}-\theta),\ \text{for}\ \tau>\tau_j.$$

$$y=W/y_0:\quad \partial\theta/\partial y=0;$$

$$S=(Q_1+Q_2)/(c_0\Delta T_0),\quad \sigma_Q=Q_1/(Q_1+Q_2),\quad \sigma_E=E_1/(E_1+E_2),$$

$$\sigma_k=k_1/(k_1+k_2),\quad \xi=\frac{\Delta T_0(E_1+E_2)}{[R(T_0+\Delta T_0)]^2},\quad \beta=\frac{R_0(T_0+\Delta T_0)}{E_1+E_2},$$

$$r_1=t_0k_1\ \exp(-\sigma_E/\beta)=t_0k_1\ \exp[-E_1/(RT_M)],$$

$$r_2=t_0k_2\ \exp[-(1-\sigma_E)/\beta]=t_0k_2\ \exp[-E_2/(RT_M)]. \tag{12}$$

The quantities r_1, r_2 have a meaning of ratios of the temporal scale t_0 to the characteristic time to the ith reaction t_{ri} at $T=T_{max}$: $r_i=t_0/t_{ri}$. The parameter S determines the ratio of the adiabatic temperature rise $\Delta T_{ad}=(Q_1+Q_2)/c_0$ to the characteristic scale of temperature variation ΔT_0. The parameter l_0 determined the characteristic size of the heated region during the time t_0. The coefficients ν_x and ν_y in Eq. (7) are the scale factors characterizing the role of thermal conductivity along the axes $0X$ and $0Y$. A high value of activation energy $E\gg RT$, i.e., $\beta\ll1$, is inherent in the combustion process [26,27]. Then $\beta\xi\le1$.

In condensed systems of the types metal–carbon, metal–boron, etc. densities of a charge of a stoichiometric composition and of a final product differ slightly. Due to the difference in heat capacities and thermal conductivities of the charge and final products a linear approximation $\bar{c}=\bar{c}_1(1-\eta_1)+\bar{c}_2(\eta-\eta_2)+c_3\eta_2$, $\bar{\lambda}=\bar{\lambda}_1(1-\eta_1)+\bar{\lambda}_2(\eta_1-\eta_2)+\bar{\lambda}_3\eta_2$ was used in Eq. (10).

The problem, Eqs. (7)–(12) was solved numerically using finite-difference methods. The kinetic Eqs. (8) and (9) were integrated by the fourth-order Runge–Kutta method. A two-dimensional nonlinear equation of heat conduction with the source, Eq. (7), was solved by a conservative implicit finite-difference scheme of the order $0(h^2+\Delta\tau)$ using the method of splitting along the directions [18].

3.7. Substantiation of initial data for a two-stage reaction

As has been noted above, various modes of combustion in a two-stage reaction differ slightly from each other and from a one-stage reaction by external features (the rate of combustion, temperature profile). In calorimetric measurements a thermal effect represents a total quantity $Q=Q_1+Q_2$ and the activation energy E refers to the leading stage of the combustion process. For the majority of systems of the type "high-melting metal (Ti, Zr, Ta, Nb)–boron or carbon" the heat of formation of the product (boride, carbide) is within

the limits Q = 2500–4000 kJ kg^{-1} [12], the adiabatic combustion temperature T_{ad} = 2500–3000 K [28].

At the porosity of the charge mixture and the product 50%, characteristic values of the thermophysical parameters are: $\rho = 2 \times 10^3$ kg m^{-3}, $c_0 \sim 10^3$ J kg^{-1} K^{-1}, $\lambda_0 \approx 15$ W m^{-1} K^{-1} [29]. By virtue of this we take T_0 = 300 K, T_{ad} = 3000 K, Q = 2700 kJ kg^{-1}. The activation energy of the chemical reaction is SHS of high-melting compounds lies within the range E = 120–300 kJ mol^{-1} [30,31], which coincides with the range of the activation energy of solid-phase diffusion in the product layer [11]. We take the value E = 170 kJ mol^{-1} for the compound TiB_2 as characteristic [11,32]. A typical value of the combustion rate for the "metal–carbon", "metal–boron" systems is $u \sim 1$ cm s^{-1}.

In the case of a one-stage reaction $A_1 \rightarrow A_2$ at the given values of the parameters it follows from the Zeldovich–Frank–Kamenetskii formula (6) that $k \sim 10^5$ s^{-1}, then $r = kt_0 \times \exp[-E/(RT_{max})] \sim 100t_0$, i.e., $t_r = 10^{-2}$ s. Assuming $t_0 = 10$, $t_r = 0.1$ s, $x_0 = y_0 = 2$ mm, we obtain the following values of the dimensionless complexes: $\beta = 0.147$, $\xi = 6.134$, $\nu_x = \nu_y = 0.1875$, S = 1.

The criterion $\mu = 9.1\gamma - 2.5\beta$ [33], which characterizes the loss of stability of a plane front of the combustion wave with a one-stage reaction, lies near the boundary between stationary and self-oscillating modes ($\mu = 1.1$).

We consider a two-stage reaction $A_1 \rightarrow A_2 \rightarrow A_3$ proceeding with about the same parameters, i.e., the observed activation energy, heat release, and combustion rate. In the "fusion" mode ($0.5 < \sigma_E < 1$ [5]) the combustion rate is determined by the first reaction which has the largest activation energy, and the total heat release [19]. In this case $E_1 = E$ = 170 kJ mol^{-1}, $Q = Q_1 + Q_2 = 2700$ kJ kg^{-1}, $k_1 \sim 10^5$ s^{-1}, $r_1 = 10$ (at $t_0 = 0.1$ s). Taking $\sigma_E = 0.7$, $\sigma_Q = 0.3$, $\sigma_k = 0.97$, we obtain $E_2 = 72.9$ kJ mol^{-1}, $\beta = 0.103$, $\xi = 8.76$, $r_2 = 15$.

In the "control" mode, where $(\sigma_Q + \sigma)/(1 + \sigma_Q + 2\sigma) < \sigma_E < 0.5$, where $\sigma = T_0/\Delta T_0$ [5], the combustion rate is determined by the second reaction proceeding with its own thermal effect at the adiabatic temperature [19]. In this case we observed activation energy refers to the second reaction $E_2 = E$ = 170 kJ mol^{-1}. At $\sigma_E = 0.3$, $\sigma_Q = 0.05$, $\sigma_k = 0.5$ [19] we have $E_1 = 72.9$ kJ mol^{-1}, $k_2 = 9 \times 10^4$ s^{-1}, $\beta = 0.103$, $\xi = 8.76$, $r_2 = 10$, $r_1 = -490$.

In the "separation" mode ($0 < \sigma_E < (\sigma_Q + \sigma)/(1 + \sigma_Q + 2\sigma)$ [5]) the rate of the combustion wave propagation corresponds to the situation when only the first reaction with its temperature and heat release takes place [19]. The observed activation energy refers to the second reaction proceeding in the mode of induction $E_2 = E$ = 170 kJ mol^{-1}. Taking $\sigma_E = 0.3$, $\sigma_Q = 0.07$ [19], $\sigma_k = 0.1$, we obtain $k_1 = 9.10^4$ s^{-1}, $r_2 = 2$, and the values of β and ξ are the same as in previous cases.

We assume that in employment of the high-speed

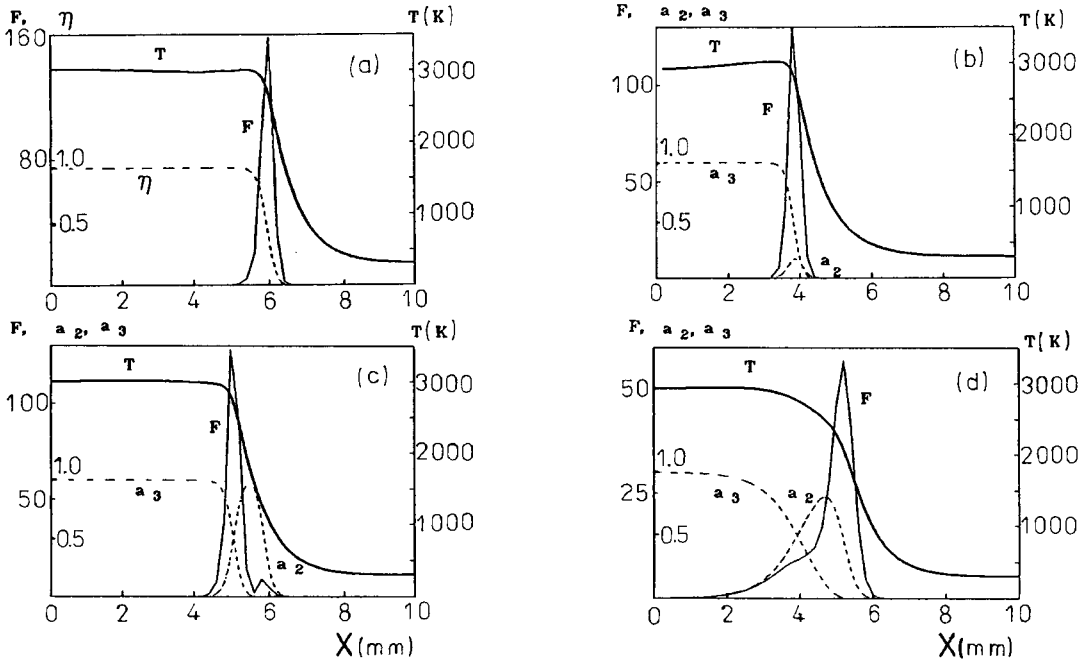

Fig. 5. Distribution of temperature heat release rate and volumetric fractions of intermediate (a_2) and final ($a_3$0 products in a SHS-wave: (a) one-stage reaction; (b)–(d) two-state reaction; mode of fusion (b), control (c), separation (d).

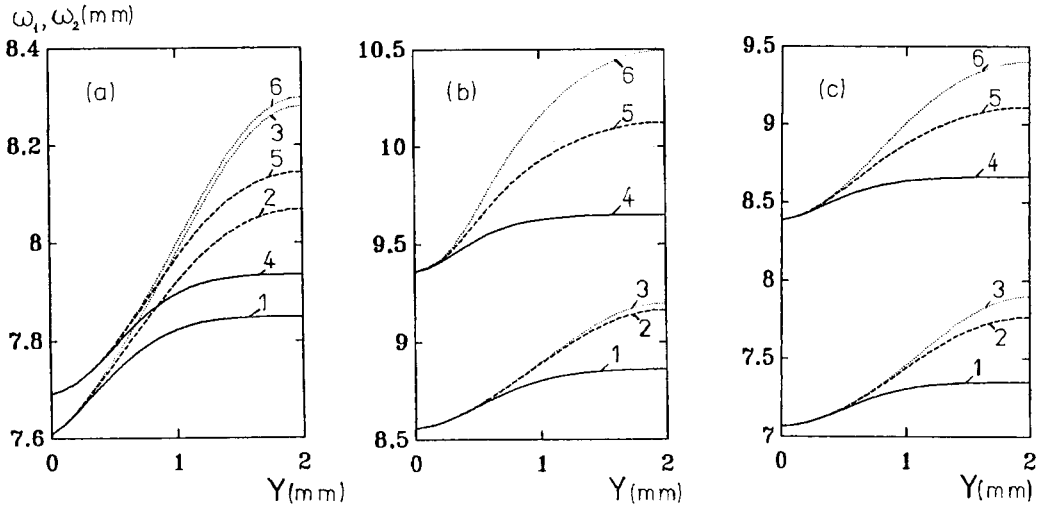

Fig. 6. Position of the fronts of reactions I (ω_1) and II (ω_2) in quenching for a two-stage reaction in the modes of fusion (a), control (b), and separation (c): 1, 2, 3) ω_1; 4, 5, 6) ω_2; for (a), (b): 1 and 4, $t = 0.025$ s; 2 and 5, 0.05 s; 3 and 6, 0.6 s; for (c): 1 and 4, $t = 0.025$ s; 2 and 5, 0.075 s; 3 and 6, 0.6 s.

water jet for cooling a burning specimen the coefficient of heat transfer on the boundary $Y = 0$ is $\alpha \sim 10^5$ W m^{-2} K^{-1} [29]. The specimen thickness is 2 mm.

3.8. Numerical investigation

The calculated structures of the combustion front for a one-stage reaction and a two-stage reaction proceeding in the "fusion", "control", and "separation" modes for the above given parameters are shown in Fig. 5. The combustion rates for all regimes are close. The temperature profiles in the modes of "fusion" and "control" virtually do not differ from each other (Fig. 5a–c). In the "separation" mode the temperature in the combustion wave changes smoother compared to the previous cases (Fig. 5d). The presence of a noticeable layer of the intermediate product is characteristic for a two-stage reaction in the modes of control and separation (Fig. 5c, d). A mean thickness of this layer Δx_2 was estimated by the size of the region of the intermediate product in which the product concentration is one-half of a maximum. In the separation mode $\Delta x_2 \simeq 1.6$ mm with a concentration $a_2 < 0.8$. In the mode of control the fraction of the intermediate product is close to unity in the layer with a thickness $\simeq 0.85$ mm. In the mode of fusion a small amount of substance A_2 ($a_2 \leq 0.2$) is observed in the zone with a width $\simeq 0.5$ mm (Fig. 5b). This is caused by the fact that in the fusion mode in contrast to the modes of control and separation, reaction II proceeds faster than reaction I since it has a lower activation energy and higher heat release. The results of numerical investigation of quenching of the burning specimen with a two-stage reaction are given in Figs. 6–8. The time given in Figs. 6–8 is reckoned from the moment of the onset of specimen cooling. It is convenient to describe the change in the position and shape of the front of reactions I and II in quenching by the quantities

$$\omega_{1,2}(Y, t) = h\int_0^L \eta_{1,2}(X, Y, t)\,\mathrm{d}X,$$

which have the dimensions of length (Fig. 6).

3.8.1. Fusion mode

It is found that in quenching of the specimen burning in the mode of fusion of a two-stage reaction, the distance between the front of reactions I and II decreases by about 4 times on a noncooled surface (Fig. 6a). On the cooled surface (at $Y = 0$) an initial position of the fronts of reactions is fixed. Combustion continues in the depth of the specimen. The first reaction ceases quicker than the second reaction and in this case the intermediate product is consumed. It is seen from Fig. 7a that on the cooled surface the volumetric fraction of the intermediate product decreases slightly from 0.194 to 0.18. With a distance from the cooled surface the concentration of the intermediate product decreases sharply: to 0.04 at $Y = 2$ mm. A mean width of the region containing product A_2 is ≈ 0.4 mm. Hence, it is very difficult to find the intermediate product after quenching, its concentration is 5 times smaller than that in the combustion wave before quenching.

In the modes of control and separation the first reaction has a lower energy of activation and proceeds faster than reaction II. By virtue of this fact, in

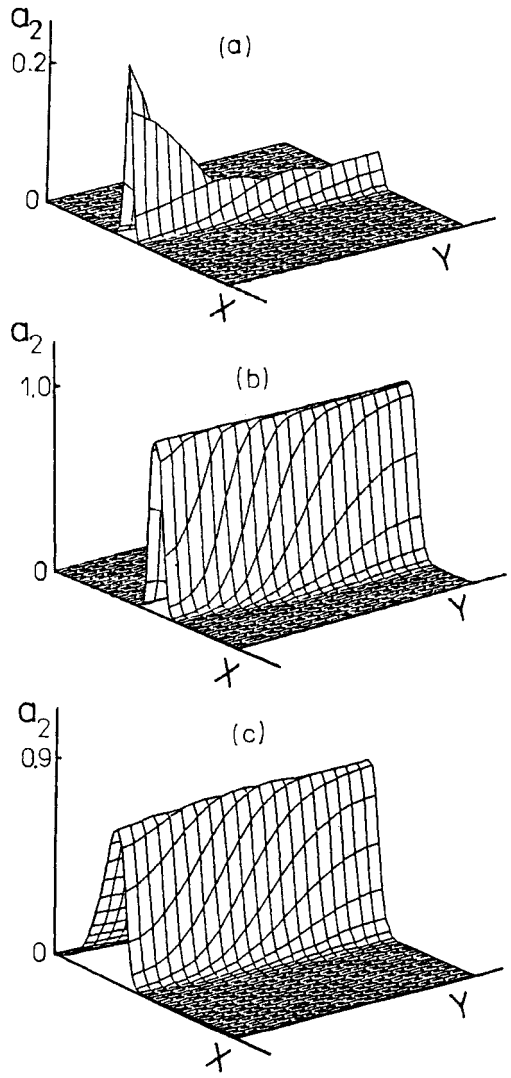

Fig. 7. Spatial distribution of a volumetric fraction of an intermediate product (a) in a quenched SHS-specimen in a two-stage reaction in modes of control (a_2), fusion, and separation (c).

quenching of an SHS-specimen the distribution of the intermediate product changes qualitatively.

3.8.2. Control mode

In quenching the positions of the fronts of reactions I and II in the combustion wave are arrested on the cooled side of the specimen ($Y = 0$). On the noncooled edge $Y = 2$ mm, starting from the onset of quenching to complete cessation of combustion the front of the first reaction passes the distance of about 2.5 times larger than that passed by the front of reaction II (Fig. 6b). This is cased by the fact that the second reaction stops quicker than the first due to a higher activation energy. It is found that the concentration of the intermediate product is constant over the width of the specimen and is close to unity (Fig. 7b). A mean width of the layer of the intermediate product on the noncooled edge of the specimen is $\Delta x_2 \approx 1.3$ mm (Fig. 7b).

Fig. 8 presents spatial temperature distribution in quenching of the specimen burning in the control mode. A sharp temperature drop occurs on the cooled surface $Y = 0$ and in the preheat zone. This leads to a noticeable reduction of the heat release rate in the zone of reaction II (Fig. 9). At $t = 0.15$ s a temperature on the noncooled surface $Y = 2$ mm is still close to adiabatic (Fig. 5d), but the heat release rate in the zone of reaction II has already become smaller than the value before onset of cooling. This is associated with intense heat removal along the axis $0Y$ which leads to stopping of the front of reaction II, and with a further decrease in temperature to ceasing reaction I.

The rate of the temperature drop $V_0 = -\partial T/\partial t$ decreases with an increase in the time of specimen cooling from 2.75×10^4 at $t = 0.025$ s to 8.10^3 K s^{-1} at $t = 0.15$ s (Fig. 10). In this case the region with a maximum value of the cooling rate shifts into the depth of the specimen and reaches the noncooled edge at $t \approx 0.05$ s from the instant of the onset of quenching. A negative value of V_0 (Fig. 10) corresponds to heating of substance in the regions where the heat still releases due to chemical reactions. In the modes of fusion and separation the evolution of spatial distribution of the temperature drop rate and its value at different time instants are close to those observed in the control mode.

Thus, a noticeable amount of the intermediate product A_2 is arrested in quenching the SHS-specimen with two-stage interaction of components proceeding in the control mode.

In the separation mode there exists a thick layer of the intermediate product. A slight increase in the thickness of the intermediate product layer on the noncooled edge of the specimen compared to the cooled surface is observed in quenching of this mode. The two reactions stop almost simultaneously (Fig. 6c). It is seen in Fig. 7c that the concentration of the intermediate product on the noncooled surface somewhat increases from 0.8 to 0.9 and this can be detected by the methods of microstructural analysis, X-ray diffraction and others.

Thus, numerical studies showed that the method of high-speed cooling of the SHS-specimen makes it possible to arrest a noticeable amount of the intermediate product in the case of a two-stage SHS-reaction wave propagating in the control or separation mode. Consequently, the quenching method which gives the coefficient of heat transfer $\alpha \gg 10^5$ W m^{-2} K^{-1} on the cooled surface (an impinging water jet), makes it possible to determine the mechanism of phase and struc-

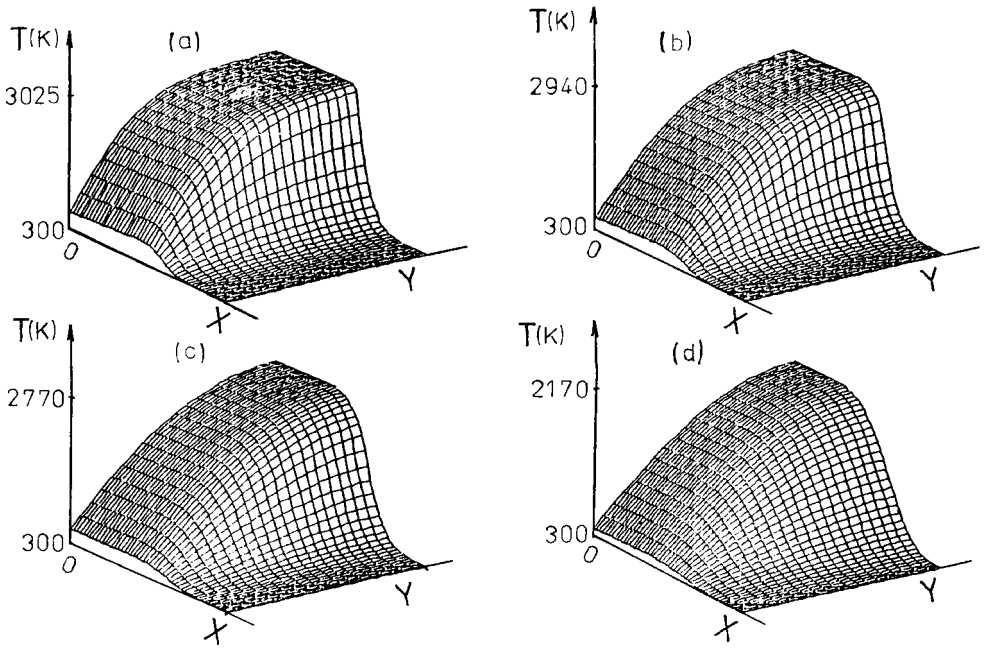

Fig. 8. Evolution of a temperature field in quenching of an SHS-specimen (control mode): (a) t = 0.025 s; (b) 0.05 s; (c) 0.075 s; (d) 0.15 s.

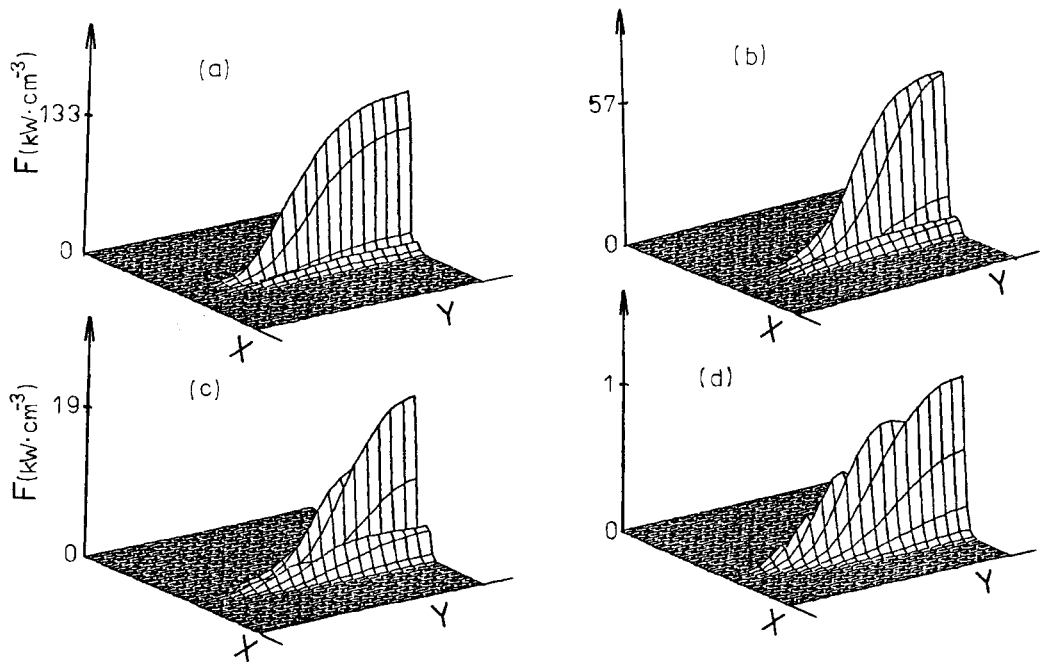

Fig. 9. Evolution of the field of heat release rate in quenching of an SHS-specimen (control mode): (a) t = 0.025 s; (b) 0.05 s; (c) 0.075 s; (d) 0.15 s.

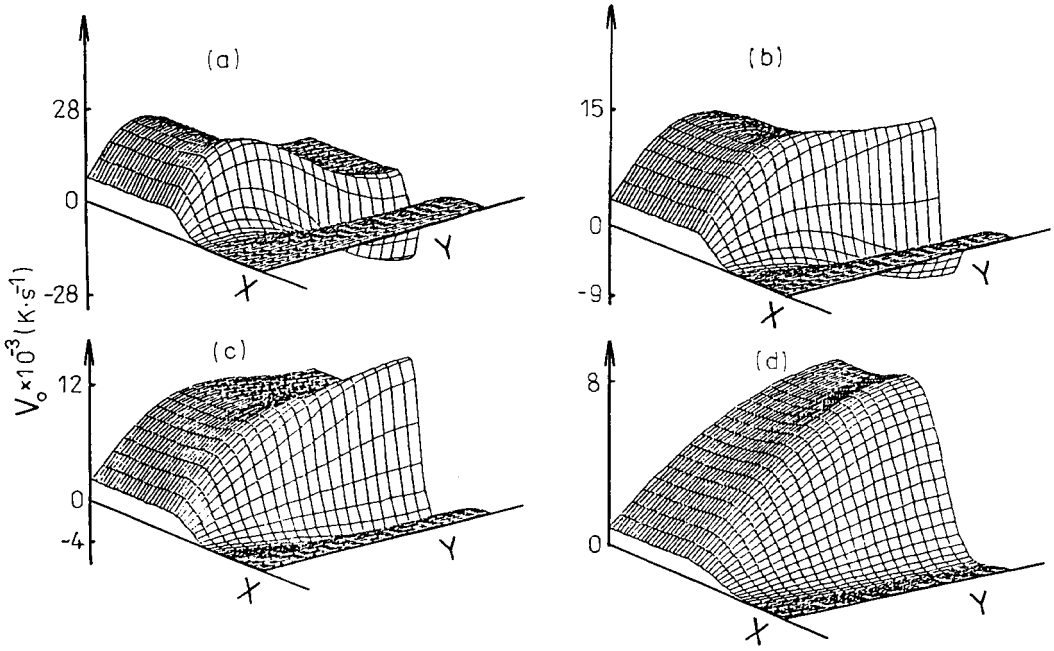

Fig. 10. Evolution of the field of cooling rate in quenching of an SHS-specimen (control mode): (a) $t = 0.025$ s; (b) 0.05 s; (c) 0.075 s; (d) 0.15 s.

ture formation in SHS. In the fusion mode the amount of the intermediate product arrested by quenching is small. In this case the determination of the mechanism of interaction in the SHS-wave by quenching will depend on the sensitivity of the methods used for the analysis of a quenched specimen.

4. Experiment

Numerical modelling made in the previous section showed a theoretical possibility to arrest the state of both final and intermediate products of reactions in an SHS-wave. In this paper we also present an experimental implementation of fast quenching of the SHS-specimen with a Ti–C mixture by a high-speed impinging water jet. A basic part of experimental equipment is shown in Fig. 11. Cooling water is fed by a positive-displacement pump to the nozzle of a round or a rectangular cross-section. The inlet part of the nozzle is shaped to eliminate jet disbalances at the outlet.

A specimen which had a shape of a cylindrical tablet with a diameter 25 mm and thickness 2–5 mm was placed in a special chamber. A reverse side of the specimen was thermally insulated from the chamber. An inlet of the chamber with the specimen was closed by a special gate protecting the specimen from the jet effect. The distance between the inlet cross-section of the nozzle and the cooled surface was ≈ 40 mm.

The specimen was prepared from the mixture of Ti and C powders, in some experiments Ni was used as an inert additive. Use of an inert additive and the stoichiometric composition of the mixture allow one to vary temperature and rate of reaction and also heat

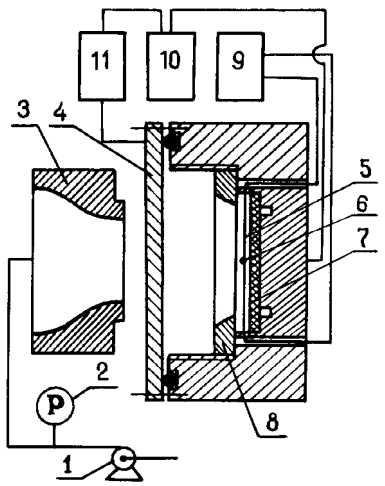

Fig. 11. Device for quenching of SHS-specimens by an impinging water jet. 1, water pump; 2, manometer; 3, nozzle; 4, gate; 5, specimen; 6, thermocouple; 7, ceramic insulator; 8, ring; 9, memory storage oscillator; 10, device for initiating SHS-reaction; 11, device for gate control.

release in the wave of synthesis. The powders were premixed in a mechanical stirrer for several hours and then tables were made in the press-form. Pressure of pressing was taken so that the density of specimens amounted to $50 \pm 5\%$ of theoretical. A tungsten–rhenium thermocouple, made of ~100 μm thick wire, was embedded in a diametral section of the specimens. In different series of experiments the depth of embedment varied along the height of the specimen to evaluate the quenching rate at different distances from the cooled surface.

Before the experiment the specimen was placed in the device and fixed by a special ring, the leads of the thermocouple were connected to the inlet of the memory-storage oscillograph to register temperature during cooling. Reaction was initiated by local heating of the edge of the specimen by a current pulse through special electrodes. The same pulse switched on the gate control unit through a special circuit. The time of delay of gate opening was selected so that the gate was opened when the combustion wave reached the place where the thermocouple was embedded. After the gate was opened, a high-speed jet impinged on the specimen surface at a right angle thus cooling it. In this process temperature variation was registered on the oscillograph screen. Some examples of thermograms recorded in the experiments are given in Figs. 12 and 13.

The experiments, the results of which are presented in Fig. 12, were made for the specimens of nonstoichiometric composition Ti–C with an excess content of titanium which amounted to ~10 wt%. We should mention some general specific features inherent to all data. A sharp decrease in temperature takes some time after the gate open. This is caused, first, by a finite time of its opening (~0.1–0.15 s) and, second, by the fact that at the initial stage of quenching a considerable portion of heat is spent to compensate the heat released in the SHS-reaction. As is shown, the reaction ceases at the moment when the temperature becomes close to the temperature of the liquid phase (Ti, ~1900 K) crystallization. Then the cooling rate attains a calculated value ($\sim 10^4$ K s^{-1}). With a distance from the cooled surface the quenching rate decreases

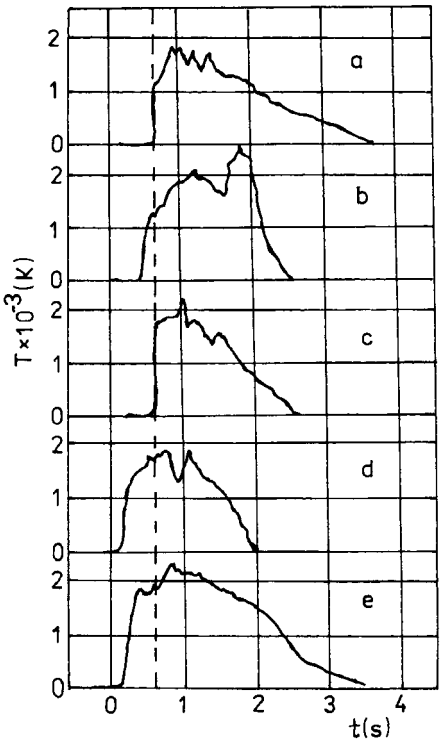

Fig. 12. Dependence of temperature variation on time in quenching SHS in the Ti–C mixture with excess 10 wt% of Ti. (a) round nozzle, $d = 2$ mm, (b)–(e) rectangular nozzle; 18 × 18 mm; dashed line, start of gate opening.

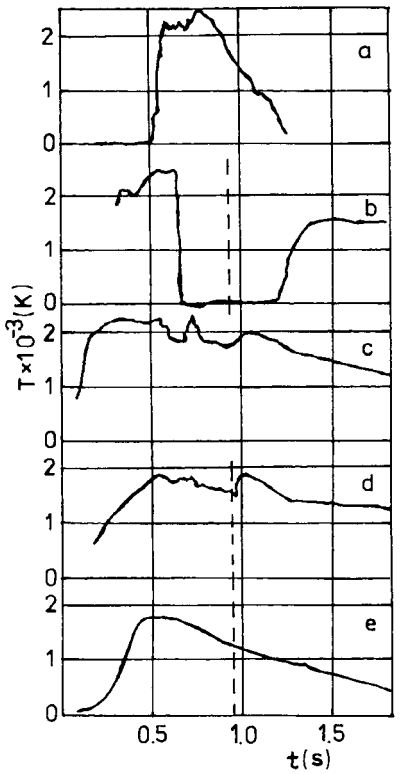

Fig. 13. Dependence of temperature variation on time in quenching SHS by an impinging jet issuing from a rectangular nozzle. Start of gate opening at $t = 0.5$ s; dashed line, cessation of cooling by a jet. (a) Ti + 0.6Si mixture; depth of thermocouple embedding $\delta = 0.7$ mm; (b) Ti + 0.5C mixture; thermocouple on the surface; (c) Ti + 0.5C mixture; $\delta = 1.2$ mm, tablet thickness 1.5 mm; (e) Ti + 0.5C mixture; $\delta = 0.7$ mm; tablet thickness 1.5 mm.

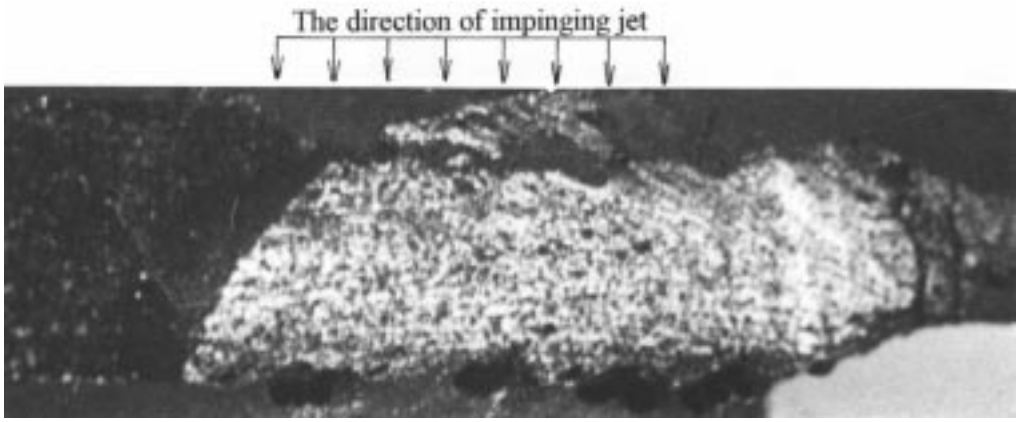

Fig. 14. Cross section of the specimen with a stopped front of the SHS-wave.

(Fig. 12c, e), that is in agreement with the results of numerical modelling. Cooling by a plane jet is much more efficient than by a jet issuing from a round nozzle (Fig. 12 a, c). This fact is likely to be explained by a larger nonuniformity in the distribution of the heat transfer coefficient over the surface of the specimen in the second case. An increase in the specimen thickness leads to an increase in the heat release rate in the fast-reaction zone and, as a consequence, to a decrease in the efficiency of quenching (Fig. 12b), and in some cases to impossibility to stop the front at the given parameters of the jet [34,36,37]. As is shown by calculations, the geometry of the specimen used in the experiments stipulates nonuniformity of the heat release along the motion of the SHS-reaction front with gradual increase to a maximum at $x \sim 0.7d$ and decrease at the end point. In this sense, optimum cross-sections from the viewpoint of fast quenching are initial and final sections of the specimen.

In the experiments the mode of cooling, when the time of interaction between the jet and the surface was limited by certain time intervals, was also used. In this case variation of temperature during quenching was more complex. Thus, in the case when the thermocouples are positioned directly on the cooled surface (Fig. 13b) very fast cooling of the specimen surface (the cooling rate $\geq 10^6$ K s^{-1}) was registered. On cessation of the effect of the cooling jet, temperature again increases considerably due to heat supply from the deep layers of the specimen. This mode of quenching offers interesting possibilities for studying phase and structure formation in the after-burn zone of the SHS-wave. In this mode the quenching rate is also dependent on the position of the thermocouple over the depth of the specimen (Fig. 13d, e) and on its thickness (Fig. 13c). As it should be expected, the effect of the heat release of the reaction is substantial. This is confirmed by Fig. 13a which illustrates the results of the experiments with the specimen made from the mixture Ti + 0.6Si, where the reaction is much lower.

As a whole, the results of the experiments are in a satisfactory agreement with the numerical calculations. It should, however, be noted that quenching with a rather high rate was attained in experiments with jet velocities not exceeding 30 m s^{-1}. This fact provides grounds to assume a substantial role of the vaporization processes (besides a convective factor) which were not considered in calculations. The estimates made by the generalized relations, the experimental data on a critical heat flux on the heater cooled by a liquid jet known at present [42–45] give the values of the heat flux that by the order of magnitude are somewhat smaller than those necessary for fast quenching of the SHS-reaction. This is likely to be associated with the specifics of the heat source which in the given case is a propagating thermal wave, whereas the earlier data were obtained for a uniformly heated disk. Superhigh temperatures of the specimen surface in SHS are also likely to be an important fact. Fig. 14 presents a cross-section of the specimen Ti + 0.5C with the stopped combustion front. In quenching, combustion ceases quickly on the cooled surface and the stopped front of the combustion wave has an arched shape thus indicating a delay of reaction stopping in the depth of the specimen compared to near-surface layers, as was shown by numerical calculations.

5. Conclusions

1. Numerical calculations of temperature fields, phase, structural and chemical transformations in quenching of one- and two-stage reactions showed the possibility of obtaining the cooling rate $\sim 10^4$ K s^{-1} by convective heat transfer between the specimen

and the impinging water jet. This makes it possible to arrest a high-temperature state of the substance in the fast-reaction and after-burn zones for a one-stage reaction. The proposed technique allows also to arrest noticeable quantities of intermediate products in the control and separation modes for a two-stage reaction. At the same time in the fusion mode the fraction of the intermediate product fixed by quenching is much smaller.

2. Except for the possibility of attaining a rather high cooling rate, the proposed technique compares favourably with the widely used means of stopping the combustion front in a massive copper block by the convenience of controlling the quenching rate and also the place and time of the onset of quenching. In this case, the structure of the combustion wave is less distorted due to a substantial decrease in the time of extinction.
3. Experimental implementation of the method of fast stopping of the combustion front by the impinging water jet showed a satisfactory agreement with the computational relations. However, the possibility of SHS quenching obtained at much lower velocities of a jet than it was assumed in modelling of this process provides grounds to assume a determining role of the vapourization processes which were not taken into account in calculations.

Acknowledgement

The authors express deep gratitude to the Fundamental Research Foundation of the Republic of Belarus for financial support (Grant No. T16-221).

References

[1] A.S. Mukasiyan, E.V. Bukreev, B.M. Khusid, B.B. Khina, A.S. Rogachev, A.G. Mershanov, I.P. Borovinskaya, Structural macrokinetics of interaction between titanium and nitrogen in the mode of combustion, Preprint No. 10 of the Institute of Heat and Mass Transfer of the Academy of Sciences of BSSR, Minsk, ITMO AN BSSR Press (1991).
[2] I.P. Borovinskaya, A.G. Merzhanov, A.S. Mukasiyan, A.S. Rogachev, B.B. Khina, B.M. Khusid, Macrokinetics of structure formation during filtration combustion in the titanium–nitrogen system, Dokl. Phys. Chem. 322 (4/6) (1992) 78–83.
[3] A.S. Rogachev, A.S. Mukasiyan, A.G. Merzhanov, Structural transformations in gasless combustion of the titanium–carbon and titanium–boron systems, Dokl. AN SSSR 297 (6) (1987) 1425–1428.
[4] A.G. Merzhanov, Self-propagating high-temperature synthesis, in: Y.M. Kolotyrkin (Ed.), Physical Chemistry—Modern Problems, Khimiya Press, Moscow, 1983.
[5] V.S. Berman, Y.S. Ryazantsev, Asymptotic analysis of stationary propagation of the front of a two-stage consequitive exothermal reaction, Prikl. Mekh. Tekh. Fiz 1 (1973) 75–88.
[6] V.S. Berman, Y.S. Ryazantsev, V.M. Shevtsova, Nonstationary propagation of a two-stage consequitive reaction in a k-phase, Fiz. Goren. Vzryva 17 (6) (1981) 72–77.
[7] B. Cantor (Ed.), Rapidly Quenched Metals, Metallurgiya Press, Moscow, 1983.
[8] M.E. Drits (Ed.), Properties of Elements—Handbook, Metallurgiya Press, Moscow, 1985.
[9] A.Y. Rozovskii, Heterogeneous Chemical Reactions (Kinetics and Macrokinetics), Nauka Press, Moscow, 1980.
[10] A.V. Luikov, Theory of Heat Conduction, Vysshaya Shkola Press, Moscow, 1967.
[11] G.V. Samsonov, I.M. Vinitskii, Refractory Compounds, Metallurgiya Press, Moscow, 1976.
[12] O. Kubaschewski, C.B. Alcock, Metallurgical Thermochemistry, Pergamon Press, Oxford, 1979.
[13] M.E. Drits, L.L. Zusman, Alloys of Alkaline and Alkaline Earth Metals: Handbook, Metallurgiya Press, Moscow, 1986.
[14] V.M. Borishanskii, S.S. Kutateladze, I.I. Novikov, O.S. Feslyuskii, Liquid-Metal Heat Carriers, Atomizdat Press, Moscow, 1976.
[15] N.B. Vargaftik, Handbook on Thermophysical Properties of Gases and Liquids, Fizmatgiz Press, Moscow, 1963.
[16] P. Hrysak, Heat transfer from round impinging jets to a flat plate, Int. J. Heat Mass Transfer 26 (12) (1983) 1857–1865.
[17] M. Lamvik, B-A. Iden, Heat transfer coefficient by water jets impinging on a hot surface, Heat Transfer-1982, in: Proceedings of the Seventh International Heat Transfer Conference, 1978, 3, pp. 369–375.
[18] A.B.A. Samarskii, Introduction to the Theory of Finite-Difference Schemes, Nauka Press, Moscow, 1971.
[19] B.M. Khaikin, A.K. Filonenko, S.I. Khudyaev, Propagation of flame in the course of two consequent reactions in a gas, Fiz. Goren. Vzryva 4 (4) (1968) 591–600.
[20] H.F. Kopman, Theoretical modelling of coal flames, Combust. Sci. Techn. 2 (2/3) (1970) 149–159.
[21] G. Joulin, P. Clavin, Asymptotic analysis of a premixed laminar flame governed by a two-step reaction, Combust. and Flame 25 (3) (1975) 389–393.
[22] A.K. Kapila, G.S. Ludford, Two-step sequential reactions for large activation energies, Combust. and Flame 29 (2) (1977) 167–176.
[23] B.M. Khaikin, A.K. Filonenko, S.I. Khudyaev, T.M. Martemiyanova, Stage combustion of nonvolatile easily-dispersed substances, Fiz. Goren. Vzryva 9 (2) (1973) 169–185.
[24] T.P. Ivleva, P.M. Krishenik, A.G. Merzhanov, K.G. Shkadinskii, On nonuniqueness of a steady-state mode of combustion of diluted gasless mixture, Khim. Fizika 9 (1983) 1259–1265.

[25] V.A. Voltpert, P.M. Krishenik, Stability of propagation of a two-stage combustion wave in the control mode, Fiz. Goren. Vzryva 22 (2) (1986) 24–31.
[26] Y.B. Zeldovich, G.I. Barenblatt, V.B. Librovich, G.M. Makhviladze, The Mathematical Theory of Combustion and Explosion, Plenum Press, New York, 1985.
[27] D.A. Frank-Kamenetskii, Diffusion and Heat Transfer in Chemical Kinetics, Plenum Press, New York, 1969.
[28] N.P. Novikov, I.P. Borovinskaya, A.G. Merzhanov, Thermodynamic analysis of reactions of self-propagating high-temperature synthesis, in: Combustion Processes in Chemical Technology and Metallurgy, OIKhF Press, Chernogolovka, 1975, pp. 174–188.
[29] B.M. Khusid, B.B. Khina, E.A. Bashtovaya, Numerical investigation of the thermal processes associated with quenching of a material in a wave of SHS, Comb. Explos. Shock Waves 27 (6) (1991) 708–714.
[30] A.I. Kirdyashkin, Y.M. Maksimov, E.A. Nekrasov, Mechanism of interaction between titanium and carbon in a combustion wave, Fiz. Goren. Vzryva 17 (4) (1981) 33–36.
[31] A.B.A. Zenin, A.G. Merzhanov, G.A. Nersisyan, Study of heat wave structure in SHS-processes (on an example of synthesis of borides), Fiz. Goren. Vzryva 17 (1) (1981) 79–90.
[32] E.A. Nekrasov, Theory of diffusion combustion of heterogeneous systems with condensed products, Doctoral Dissertation (Phys. Math.), Tomsk (1990).
[33] K.G. Shkadinskii, B.I. Khaikin, A.G. Merzhanov, Propagation of a pulsating exothermic reaction front in the condensed pahse, Comb. Explos. Shock Waves 7 (1) (1971) 15–22.
[34] V.V. Kulebyakin, A.V. Karpechenko, Nonstationary heat transfer in quenching of substance state in an SHS-wave by an impinging jet, in: Proceedings of the International School-Seminar, Rheophysics and Thermal Physics of Nonequilibrium Systems. Part 2. Kinetic Processes in Condensed Media, ANK ITMO AN BSSR Press, Minsk, 1991, pp. 72–74.
[35] A.G. Merzhanov, A.S. Rogachev, A.S. Mukasiyan, B.M. Khusid, Macrokinetics of structural transformations during gasless combustion of titanium and carbon mixture, Comb. Explos. Shock Waves 26 (1) (1990) 92–101.
[36] B.M. Khusid, B.B. Khina, E.A. Bashtovaya, Simulation of the process of stopping a combustion front in an SHS-wave, in: Mathematical Simulation of Technological Processe4 s of Material Pressing, Extended Abstracts of the All-Russian Scientific-Engineering Conference, Perm, 1990, p. 74.
[37] B.M. Khusid, E.A. Bashtovaya, B.B. Khina, On the possibility of arresting a combustion front of an SHS-wave, in: Rhinokinetics and Convection of Structurising Compositions, ITMO AN BSSR Press, Minsk, 1990, pp. 72–81.
[38] E.A. Nekrasov, Y.M. Maksimov, M.K. Ziatdinov, A.S. Sheinberg, Influence of capillary spreading on propagation of a combustion wave in gasless systems, Fiz. Goren. Vzryva 14 (5) (1978) 26–32.
[39] R.B. Kotelnikov, S.N. Bashlykov, Z.G. Galiakbarov, Super-High-Melting Elements and Compounds, Metallurgiya Press, Moscow, 1968.
[40] V.E. Zinoviev, Thermophysical Properties of Metals at High Temperatures: Handbook, Metallurgiya Press, Moscow, 1989.
[41] V.P. Glushko (Ed.), Thermodynamic Properties of Individual Substances: Handbook, 1, AN SSR Press, Moscow, 1982.
[42] S. Faggiani, W. Grassi, Impinging liquid jets on heat surfaces, in: Proceedings of the 9th International Heat Transfer Conference, Jerusalem, 1990, 1, pp. 275–285.
[43] Y. Katto, S. Yokoya, Critical heat flux on a disk heater cooled by a circular jet on saturated liquid impinging at the center, Int. J. Heat Mass Transfer 31 (2) (1988) 219–227.
[44] S. Ishigai, S. Nakanishi, T. Ochi, Boiling heat transfer for a plane water jet impinging on a hot surface, in: Proceedings of the Sixth International Heat Transfer Conference, Toronto, 1978, 1, pp. 445–450.
[45] Y. Katto, M. Monde, Study of mechanism of burn-out in a high heat-flux boiling system with an impinging, in: Proceedings of the Fifth International Heat Transfer Conference, 1974, 4, pp. 245–249.